Datacite DOI: https://doi.org/10.5281/zenodo.438934
CrossRef DOI: http://doi.org/10.1366/0003702934067180

Fiber-Optic Time-Resolved Fluorescence Sensor for *in Vitro* Serotonin Determination

STEPHANE MOTTIN,* CANH TRAN-MINH, PIERRE LAPORTE, RAYMOND CESPUGLIO, and MICHEL JOUVET

Laboratoire de Biotechnologie, Ecole Nationale Superiéure des Mines de St-Etienne, F-42023 St-Etienne Cedex 2, France (S.M., C.T.); Laboratoire T.S.I., URA CNRS 842, Université Jean Monnet, F-42023 St-Etienne Cedex 2, France (P.L.); and Département de Médecine Expérimentale, INSERM U 52, Université Claude Bernard, F-69373 Lyon Cedex 08, France (R.C., M.J.).

@Article{1993_mottin_4,
author = {Mottin, Stéphane and Tran-Minh, Canh and Laporte, Pierre and Cespuglio, Raymond and Jouvet, Michel},
title = {Fiber optic time-resolved fluorescence sensor for in vitro serotonin determination},
journal = {Appl. Spectro.},year = {1993},volume = {47},number = {5},pages = {590-597},doi = {10.1366/0003702934067180},
keywords = {Time-resolved spectroscopy;fluorescence;serotonin;Sensor;in vitro;fluorescence lifetime;UV;optical fibre},}

Mottin, S. identifier: http://orcid.org/0000-0002-7088-4353

At pH 7 and with the excitation at wavelengths above 315 nm, previously unreported fluorescence of 5-HT (5-hydroxytryptamine) is observed. Two fluorescence bands were observed for 5-HT; the first emits at around 390 nm with an associated lifetime near 1 ns, and the other (well known) emits at 340 nm with an associated lifetime of 2.7 ns. With both static and time-resolved fluorescences, the spectral and temporal effects of the excitation wavelength were studied between 285 and 340 nm. With these basic spectroscopic properties as a starting point, a fiber-optic chemical sensor (FOCS) was developed in order to measure 5-HT with a single-fiber configuration, nitrogen laser excitation, and fast digitizing techniques. Temporal effects including fluorescence of the optical fiber were studied and compared with measurements both directly in cuvette and through the fiber-optic sensor. Less than thirty seconds are required for each measurement. A detection limit of 5-HT is reached in the range of 5 μM. Our system, with an improved sensitivity, could therefore be a possible and convenient "tool" for *in vivo* determination of 5-HT.

Index Headings: **Spectroscopic techniques; Fluorescence; Time-resolved spectroscopy; Serotonin; Optical fluorometric sensors.**

INTRODUCTION

Historically different approaches (anatomical, neurophysiological, and pharmacological) have helped to establish a relationship between the level of brain serotonin (5-hydroxytryptamine or 5-HT) and the alternation of the different states of vigilance. New techniques have offered the possibility of studying the activity of serotoninergic neurons throughout the sleep-wake cycle.[1] Methods of measuring 5-HT or 5-HIAA (5-hydroxyindoleacetic acid) levels *in vivo,* which allow the investigation of its release and metabolism, are divided into two categories, voltammetry and dialysis (push-pull perfusion).[2–4] *In vivo* voltammetry is associated with good anatomical resolution because of the small electrode sizes. Compound specificity, however, is the major limitation of the voltammetric technique.[5] Dialysis is also associated with advantages and limitations. Dialysis allows a greater specificity of compound detection, but the thickness of the dialysis probe limits anatomical resolution. In addition, the dialysis probe has a relatively short "functional" life *in vivo,* and the necessity for long time intervals between successive measurements limits the association of compound release with specific behavioral events.[6]

These limitations lead us to search for an alternative *in vivo* monitoring technique which would involve a miniature sensor characterized by rapidity, specificity, and sensitivity of measurements. In this paper, we present the feasibility of *in vitro* rapid determination of 5-HT (less than 30 seconds) by a fiber-optic chemical sensor (FOCS). The single-fiber configuration is preferred, rather than the double-fiber or multiple-fiber configuration, despite an increase in white noise associated with single fibers.[7] In addition, the injection and collection of light complicate the setup. For the possible extension to an *in vivo* sensor, the interactions between the sensor and media must be the simplest in order to miniaturize, sterilize, and minimize problems of incompatibility of materials such as the resins used for the attachment of two fibers. Detection limit sensitivity depends on experimental parameters. These parameters are critical for the magnitude of the fluorescence noise and the efficiency of the single-fiber optical coupler configuration. Specificity was investigated, and the signal produced by 5-HIAA was also characterized. Relationships between results and choice of instrumentation are discussed.

One such choice was the use of the time-resolved fluorescence technique. Such a method has been widely used in fields as diverse as molecular biology, polymer science, and solid-state physics.[8] In most cases, the aim is to provide only qualitative measurements. Nevertheless, quantitative methods appear necessary, especially when the steady-state fluorescence intensity is not sufficient.[9–11] Two approaches for quantitative applications have emerged. The first approach uses a fiber optic with the construction of an extrinsic time-resolved fluorescence optrode for remote sensing[12] and a semi-intrinsic optrode for detection of chemical compounds which have no fluorescence.[13,14] The second approach involves the field of time-resolved fluorescence instrumentation in order to obtain a rapid and simplified technique.[15,16]

Photophysical properties of 5-HT are mainly due to the 5-hydroxyindole chromophore. In order to selectively measure 5-HT by a remote sensor using optical fibers, we examined specific photophysical properties for this group with regard to indole compounds (e.g., tryptophan) and especially between 5-HT and 5-HIAA within the group of 5-hydroxyindolic compounds. Some differences in UV absorbance are found in polar solvents between simple indoles and indoles which are substituted in the

Received 14 October 1992; revision received 17 December 1992.
* Author to whom correspondence should be sent.

0003-7028/93/4705-0590$2.00/0

ring at the five position;[17] in contrast with the ^1L_a band (notation of Platt[18]), many differences occur for the ^1L_b band, such as a red shift and a decrease in the molar extinction coefficient.

Native fluorescence (called UV fluorescence) of 5-HT in neutral aqueous solutions was reported as early as 1955—namely, the excitation and emission of the 5-HT peak at 295 and 340 nm, respectively.[19] Another emission with a maximum near 550 nm (called green fluorescence) was found in strongly acidic solutions without any change in the absorption spectrum.[20] This unusual fluorescence with such a large Stokes shift is very specific to 5-hydroxy or 5-alkoxy indoles[21] and was widely used for the fluorometric assay of 5-HT.

Finally, at physiological pH levels, native UV fluorescence of 5-HT does not seem to be usable for our purpose because of the lack of specificity. Native green fluorescence of 5-hydroxyindole compounds becomes important at a pH near to 2, which is, according to our goal, difficult to exploit.

We first studied the photophysical properties of 5-HT when it was excited at the nitrogen laser band of 337 nm, despite the fact that this wavelength lies at the extreme limit of the absorption spectrum. The goal was to choose a wavelength which avoids absorption (and fluorescence) of indole compounds such as tryptophan and still allows an absorption of 5-hydroxyindolic compounds. The 337-nm excitation produces a broad blue-band fluorescence emission (maximum: 390 nm, width: 70 nm) which, to our knowledge, has not been previously reported. In addition we investigated some photophysical properties of 5-HT with a steady-state technique and with a flashlamp time-correlated single photon counting (TCSPC) technique. Actually two fluorescence bands were observed for 5-HT; the first, well known, emits at 340 nm with a lifetime of 2.7 ns, and the other emits at around 390 nm with a lifetime near 1 ns. The spectral and temporal effects of the excitation wavelength are noticeable.

An extrinsic FOCS with subnanosecond resolution and rapid evaluation of lifetime ranges has been developed with UV excitation at the nitrogen laser wavelength at 337 nm. Parent techniques have been previously described in the literature, but with visible excitation.[22] Additional technical difficulties occur when one is using UV excitation, such as the great attenuation of the fiber and the increase in fluorescence noise. Some interferences generated by the fiber fluorescence are time-filtered by using a time-resolved fluorescence technique. We describe single-fiber configuration for use at 337 nm as the excitation wavelength. This method can be applied for in-line and *in vivo* analysis when the photophysical properties of the compounds under investigation are such that they absorb in the near-UV range and fluoresce with a Stokes shift of more than 40 nm.

THEORY

If $[C^*]$ represents the concentration of excited molecules, we have the following formula:

$$\frac{d[C^*]}{dt} = -\sum_{i=1}^{n} k_i[C^*] + \gamma I_{abs} \quad (1)$$

where k_i ($i = 1, n$) are the rate constants for each mode of deactivation of the excited state, and I_{abs} is the flux of photons absorbed. γ ((mole/L)/photon) is the light efficiency for the molecular excitation.

In case of instantaneous excitation we have:

$$\frac{d[C^*]}{dt} = -\sum_{i=1}^{n} k_i[C^*]. \quad (2)$$

So we can write: $[C^*](t) = [C^*]_0 \exp(-t/\tau_m)$ with τ_m the measured fluorescence lifetime:

$$\tau_m = \frac{1}{\sum_{i=1}^{n} k_i}. \quad (3)$$

The intensity of the fluorescence observed at a time t after excitation is expressed by:

$$F(t) = k_F[C^*] = [C^*]_0 \exp(-t/\tau_m)/\tau^0 \quad (4)$$

where $k_F = 1/\tau^0$, k_F is the rate constant for the emission of photons as a mode of deactivation of the excited state, and τ^0 is called the intrinsic fluorescence lifetime.

With the Beer-Lambert law, we can write: $[C^*]_0 = I_0(1-10^{-\epsilon L[C]})$ where I_0 is the number of excitation photons, ϵ the molar absorption coefficient, L the optical path, and $[C]$ the molar concentration. If the absorbance is low ($\epsilon L[C] < 0.05$) we can write:

$$F(t) \approx 2.3\epsilon L[C] I_0 \exp(-t/\tau_m)/\tau^0. \quad (5)$$

From this equation, the integrated fluorescence intensity (H) is

$$H([C]) = \int_0^\infty F(t)\, dt \approx \frac{2.3\epsilon L I_0 \tau_m}{\tau^0}[C]. \quad (6)$$

H is a linear function of the concentration for small absorbances.

With our laser fluorometer, the fluorescence lifetimes are evaluated by the method based on the numerical convolution of the instrument response function (IRF) and a least-squares optimized comparison with the experimental signal.[22] The 512 points of the IRF are convoluted with a single exponential decay. The result is compared to the experimental fluorescence response between 1 and 10 ns by means of an unweighted χ-squared test. The χ-square test is a measure of the goodness of fit. But the χ-square has absolute meaning only if the weighting factors are specified. In our measurements with our laser fluorometer based upon the fast digitizing technique, the noise is not similar to the Poisson distribution, and so the variance, used to calculate the weighting factors, cannot be taken to be equal to the experimental value.[23-25] In addition, relative residues r_i are set in percent:

$$r_i = \frac{y_i - y(x_i)}{y_i} \quad (7)$$

where y_i are the experimental data and $y(x_i)$ the fitting function.

Temporal multimodal broadening is negligible in our application because of the small length of the optical fiber.[26] A small time shift of the fluorescence response is necessary because of the difference between the transit times for fluorescences collected at different wave-

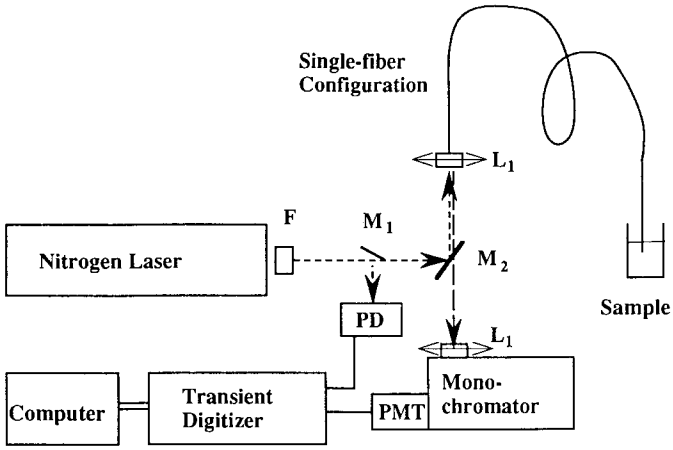

FIG. 1. Representation of the setup used for time-resolved fluorescence measurements with the optical fiber: **F**, filter; **M**, mirror; **L**, lens; **PMT**, photomultiplier; **PD**, photodiode.

lengths. This shift is due to the fiber-core refractive index change with wavelength.

MATERIALS AND METHODS

Reagents. 5-HT hydrochloride (97%) and 5-HIAA free acid (98–100%) were obtained from Sigma Chemical Co. 5-HT hydrochloride (99%) from Aldrich was also used for static fluorescence and TCSPC experiments with no noticeable change. Solutions were prepared by using commercial phosphate buffer (Merck) for solutions at pH 7. Solutions were freshly prepared each day.

Absorption Measurements. The apparatus used was a Kontron Model 860 connected to a microcomputer by RS232 to transfer data.

Steady-state Fluorescence Measurements. An LS-50 luminescence spectrometer from Perkin-Elmer was used, with 1 s as the time integration and 1- and 5-nm bandwidths for the excitation and emission monochromators, respectively.

Time-resolved Fluorescence Measurements. The time-resolved fluorescence of 5-HT at different excitation wavelengths was studied with the use of a Model 299T time-domain fluorometer from Edinburgh Instrument, equipped with a nitrogen flashlamp. The excitation and emission bandwidths were set at 10 nm and 20 nm, respectively. The TCSPC technique, however, is poorly suited to the fast measurements required for our FOCS purpose, because a count rate of less than 0.01 photoelectron per laser pulse is desirable in order to avoid distortions caused by the occurrence of more than one photoelectron per counting cycle. A specific setup using nitrogen laser excitation and a real-time method utilizing a transient digitizer was developed to overcome the TCSPC limitations.

A diagram of the experimental setup used with laser excitation is shown in Fig. 1. The nitrogen laser (Model LN120C, PRA Laser Inc., Laser Photonics Company) delivers subnanosecond pulses of 300 ps (FWHM) and 70 μJ/pulse. The 337.1-nm radiation is first filtered by a black filter (Type UG 1, Schott, France) to eliminate visible light generated by some nitrogen plasma discharges between the electrodes of the cavity. A small mirror is placed on the border of the light beam and focused on a fast photodiode (EG&G Model UV 1B), which is used as a trigger for the digitizer. The laser beam is reflected by a mirror (Model 614, Schott) identified as M_2, and focused on the optical fiber by a small lens with a focal length determined in such a way that the input aperture is less than the numerical aperture of the optical fiber. The optical fiber is a step index multimode Model PCS 1000 from Quartz et Silice (plastic-clad silica fiber optic, core-plus-cladding diameter of 1260 μm with a 1000-μm core, numerical aperture equal to 0.4). The single-fiber configuration of the FOCS uses the same fiber to transmit the excitation radiation to the sample and to guide the collected fluorescence to the detection system. The fluorescence signal goes through the mirror M_2. This mirror has a reflectance of more than 90% for wavelengths lower than 370 nm and a transmittance of more than 90% for wavelengths more than 415 nm. The fluorescence signal is focused on the entrance slit of the monochromator (Jobin Yvon) with a lens identical to that used for injection of the laser into the fiber. The fixed slits provide a 4-nm resolution. The photomultiplier (PMT) is an R3810 from Hamamatsu, with the gain selected to obtain such a response that single events are easily detected by 50-Ω input fast electronics. The voltage divider is an E850-13 MOD from Hamamatsu. The overall response time of the PMT and divider is 0.8 ns (FWHM). The main limitation of this photodetector is the saturation which occurs at a typical flux of ten photons within the time window of 1 ns. The 50-Ω output of the PMT is sent to a transient digitizer (Tektronix Model 7912 AD mainframe, Model 7A19 amplifier unit, Model 7B90P time base unit), which is triggered by the above-mentioned fast photodiode. Each individual point of the sample fluorescence decay is transferred by a GPIB bus to a microcomputer with the use of a program written by ourselves. For the time window used (10 ns), temporal memory resolution is around 20 picoseconds, i.e., much shorter than the digitizer rise-time (0.7 ns).

For measurements performed directly with cuvettes, after removal of the optical fiber, mirror M_2, and lenses L_1, the laser beam is focused after the M_1 mirror with a cylindrical lens. The cuvette is placed in front of the slit of the emission monochromator.

We have chosen a transient digitizer since it is very flexible due to its ability to account for single or multiple events as well as allowing the time-filtered fluorescence of the optical fiber and compounds. In addition, it is less expensive than a laser TCSPC system. In this paper, our aim is not to obtain the best accuracy on fluorescence lifetimes but to characterize relative concentrations within less than thirty seconds. In practice it was sufficient to collect and average signals for 25 s at 15 Hz for either instrumental or fluorescence responses.

RESULTS AND DISCUSSION

Absorption of 5-HT. In a buffer at pH 7, absorption spectra of 5-HT and 5-HIAA exhibit no measurable differences. Figure 2 (curve **a**, top) displays the absorption spectrum between 240 and 340 nm of 5-HT in the Merck buffer at pH 7. Low molar extinction, however, can be

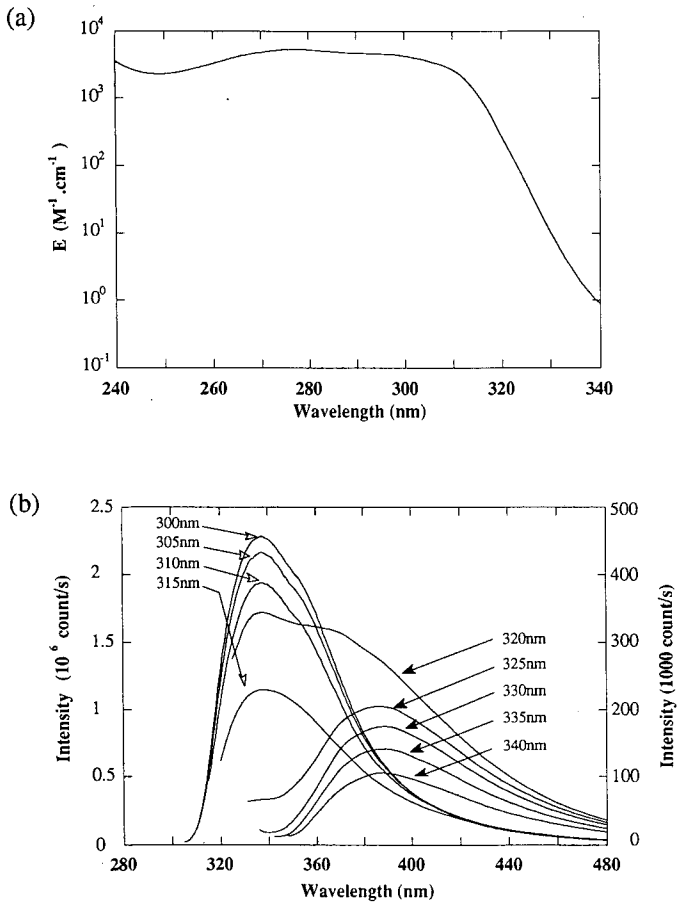

FIG. 2. Results in cuvette: (**a**, top) absorption spectrum of 5-HT in Merck buffer pH 7; (**b**, bottom) emission spectra of 5-HT fluorescence in Merck buffer pH 7 at different excitation wavelengths (concentration equal to 66 μ**M**). Black solid arrows refer to the right ordinates.

measured since 5-HT is very soluble in water. Special attention is given to molar extinction of 5-HT at 337 nm: a typical value is on the order of 2.5 $\mathbf{M}^{-1}\cdot\mathrm{cm}^{-1}$, i.e., one thousand times less than the maximum value of the ^1L_b band. Therefore, the nitrogen laser wavelength lies in the extreme limit of the absorbance of 5-HT. This fact is probably the reason why 5-hydroxyindole compounds were never studied at this wavelength.

Fluorescence of 5-HT in Cuvette. In Fig. 2 (curve **b**, bottom), the emission spectra of the 5-HT fluorescence in Merck buffer pH 7 (concentration is set at 66 μ**M**) is reported with different excitation wavelengths. When the range of excitation wavelength is less than 320 nm, emission spectra of 5-HT correspond to the well-known UV spectrum.[19] Above the 320-nm excitation wavelength, a new band appears with a maximum at nearly 390 nm and a bandwidth around 70 nm. Tryptamine (10 mM) was chosen to investigate whether a comparable phenomenon could be found for indole compounds not hydroxylated at the five position of the ring. In such a case, no fluorescence was detected for the same excitation. On the other hand, 5-HIAA, in the same conditions, exhibits the same spectral properties for its emission fluorescence (maxima and bandwidth) as compared to 5-HT. However, emission intensity of 5-HT is greater than the one of 5-HIAA by a factor of about ten.

We have investigated the time-resolved fluorescence

TABLE I. Bi-exponential analysis of 415-nm emission fluorescence of 5-HT in Merck buffer pH 7 at different excitation wavelengths (λ_{exc}).[a]

λ_{exc} (nm)	α_1 (%)	t_1 (ns)	Δt	α_2 (%)	t_2 (ns)	Δt	χ^2	DW	f_1	f_2
285	18.9	0.55	0.02	81.1	2.8	0.01	1.20	1.54	4.4	95.6
295	18.8	0.87	0.02	81.2	2.6	0.05	1.14	1.85	7.2	92.8
300	24.0	0.96	0.03	76.0	2.8	0.01	1.27	1.61	9.7	90.3
305	31.6	0.85	0.07	68.4	2.6	0.04	1.11	1.79	13.1	86.9
310	47.8	0.85	0.01	52.2	2.8	0.02	1.51	1.36	21.6	78.4
315	75.2	1.00	0.03	24.8	3.2	0.10	1.11	1.73	48.8	51.2
320	79.3	0.84	0.02	20.7	1.8	0.09	1.23	1.82	64.0	36.0
325	98.5	0.99	0.01	1.5	13.3	6.8	1.12	1.90	83.0	17.0
335	96.0	1.00	0.01	4.0	6.5	1.4	1.09	1.90	79.4	20.6

[a] Note: α_i are the pre-exponential weighting factors in percent; t_i are the decay times in ns; Δt are the estimated errors on t_i from the Edinburgh Instrument program; χ^2 is the reduced χ-square; DW is the Durbin Watson parameter; f_i are the fractional contributions to the total emission for each component:

$$f_i = \frac{\alpha_i t_i}{\sum_i \alpha_i t_i}.$$

of 5-HT at 415-nm emission wavelength and at different excitation wavelengths from 285 to 335 nm with the flash-lamp fluorometer. The emission wavelength was chosen at 415 nm in order to totally avoid the Raman band of water and to remain near the best signal for the 390-nm peaked fluorescence band. The 5-HT concentration was set at 500 μ**M**. No concentration quenching was found for this concentration. With the Edinburgh Instrument software, bi-exponential fits gave best results. Table I shows the bi-exponential analysis where the pre-exponential weighting factors (in percent) are α_i, the lifetimes are t_i (in ns), the estimated errors on t_i of the Edinburgh Instrument program are Δt, the reduced χ-square is χ^2, the Durbin Watson parameter is DW, and the fractional contributions to the total emission for each component are f_i:[27]

$$f_i = \frac{\alpha_i t_i}{\sum_i \alpha_i t_i}. \tag{8}$$

The first component has a decay time of approximately 1 ns and the second of 2.7 ns. With the 290-nm excitation wavelength and 340-nm emission wavelength, Chen *et al.*[28] previously reported a decay time of 5-HT equal to 2.7 ns, which corresponds to our second component. The reduced χ-square χ^2 and the Durbin Watson parameters are satisfactory except in the case of the analysis at the 310-nm excitation wavelength, which exhibits a high χ^2 and a bad DW for the bi-exponential model due to an undetermined origin. When excitation wavelength increases, the fractional contribution of the first component also increases. At the 315-nm excitation wavelength and 415-nm emission wavelength, the fractional contributions are also quite equal. Below 295 nm of excitation wavelength, the first component is too much reduced, and least-squares fitting loses its accuracy. On the contrary, above 320 nm, the second component becomes so weak that large errors occur in its lifetime calculated by least-squares fitting; the associated pre-exponential weighting factors are less than 5%, but, because of larger lifetime values, the fractional contributions are in the range of 20%.

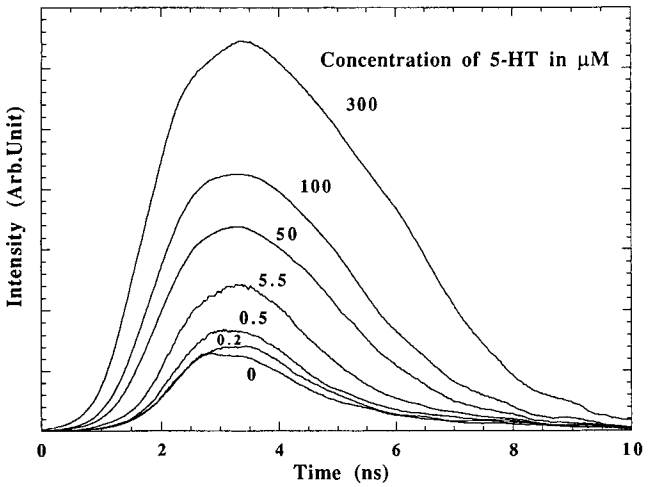

FIG. 3. Laser time-resolved fluorescence of 5-HT in Merck buffer pH 7 at different concentrations in cuvette. The emission wavelength is 430 nm with a 4-nm bandwidth.

The existence of two distinct fluorescence bands having different decay times, together with their respective intensities changing with the excitation wavelength, implies clearly that two different emitting states of 5-HT are involved. The first decays through a 1-ns lifetime and 390-nm centered emission wavelength and the other through a 2.7-ns lifetime and 340-nm centered wavelength.

With nitrogen laser excitation, the temporal dependence of the signal vs. concentration of 5-HT is clearly shown in Fig. 3. Due to the saturation of the photomultiplier restricting its linear operating range, the distortion of the fluorescence response function appears on the curve associated with 300 μM 5-HT concentration. On the other hand, at low intensities the detection is limited by parasitic fluorescence. Therefore, the analysis of life times has to take into account these two opposing limitations. In Fig. 4, experimental results and convolution calculation for 5-HT and 5-HIAA are displayed. The concentrations of 5-HT and 5-HIAA are 30 μM and 600 μM, respectively. These concentrations have been found to be optimal in our conditions in view of the above-mentioned opposing limitations. A noticeable difference between lifetimes of 5-HT and 5-HIAA was found: 1.2 $\pm$ 0.15 ns for 5-HT and 2.1 $\pm$ 0.2 ns for 5-HIAA. As for the emission intensity of 5-HT, it was found to be greater than that of 5-HIAA by a factor of twenty. The higher-range concentration of 5-HIAA, in comparison with 5-HT, does not involve an inner filtering because of the low absorption extinction coefficient of these two compounds at 337 nm. With our laser time-resolved fluorometer, the 5-HT lifetime is found to be equal to 1.2 $\pm$ 0.15 ns, which is compatible with the 1-ns value obtained with the TCSPC Edinburgh Instrument for the same excitation wavelength. For 5-HIAA, further experiments with TCSPC would be necessary to measure with accuracy its fluorescence lifetime.

Fiber-optic Time-resolved Fluorescence Sensor. *Spectral and Temporal Effects of the Optical Fiber.* Two different quartz optical fibers with high numerical apertures (0.4) were tested: "TECS fiber" from 3M, and "Quartz et Silice" fiber. With 337 nm as the excitation

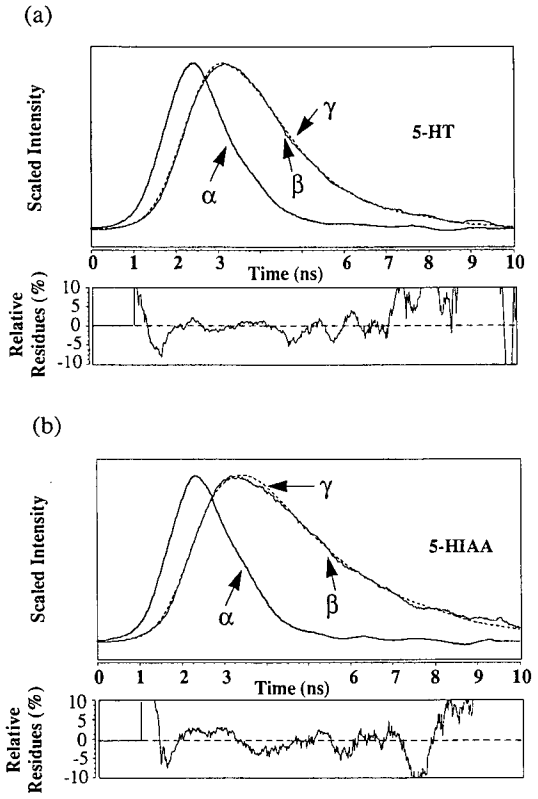

FIG. 4. Time-resolved fluorescence of: (**a**, top) 5-HT (30 μM) in Merck buffer (pH 7) in cuvette. The emission wavelength is 450 nm with a 4-nm bandwidth. The excitation wavelength is 337 nm from a nitrogen laser. Curve α: instrument response function; Curve β: emission fluorescence response; Curve γ (dotted line): calculated response with a 1.2-ns lifetime. (**b**, bottom) 5-HIAA (600 μM) with the same conditions used for part **a**, and calculated response with a 2.1-ns lifetime.

wavelength, the TECS fiber exhibits a high fluorescence in the near-UV and visible range. The Quartz et Silice fiber exhibits a much lower fluorescence level with a maxima below 400 nm. This parasitic fluorescence appears significant only at the injection of the laser into the fiber. In Fig. 5, the time-resolved fluorescence of Quartz et Silice fiber Model PCS 1000 is reported to illustrate the signal generated. A fiber length of several meters (typically 6 m) was chosen both to assess realistic use of future *in vivo* applications and to get enough separation between the fluorescence generated at the laser injection into the fiber from that collected at the tip of the fiber. However, further increasing the length of the fiber would lead to a noticeable attenuation of the laser beam. From data supplied by the manufacturer, at 337 nm and for 6.2 m of PCS 1000, the fiber transmittance is approximately 80%. For *in vivo* or in-line monitoring, this length allows the apparatus and the measurement devices to be placed in different rooms. The emission wavelength at 415 nm is chosen because the signal-to-noise ratio is at an optimum. When we consider the three principal factors (i.e., the UV excitation, the fluorescence emission, and the optical fiber use), the main advantage of time-resolved fluorescence over steady-state fluorescence is to decrease the effect of the parasitic light generated by the optical fiber by temporal separation. The time taken by light to travel the round-trip distance through 6.2 m of the fiber (L) is around 65.5 ns (see Fig. 5). At 415 and

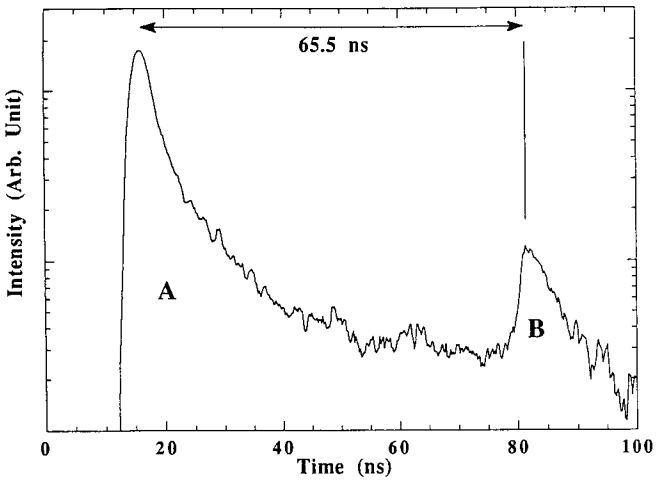

FIG. 5. Emission intensity (log scale) at 415 nm through a 6.2-m-long PCS 1000 optical fiber with the exit end (end B) dipped into the Merck buffer at pH 7. Peak *A* is due to retrofluorescence of optical fiber mainly at the laser beam injection. Retrofluorescence of the fiber tip generates peak *B*.

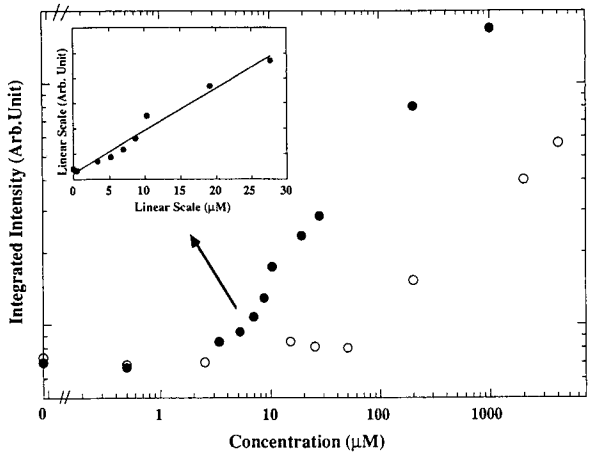

FIG. 6. Integrated intensity of emission fluorescence pulse in the Merck buffer at pH 7, guided and collected by the same optical fiber. (●) 5-HT fluorescence; (○) 5-HIAA fluorescence). The emission wavelength is 415 nm with a bandwidth of 4 nm. The excitation wavelength is 337 nm.

337 nm, the refractive indexes (n_1 and n_2) of the core fiber are, respectively, 1.467 and 1.479. The numerical aperture (NA) is 0.4. With the geometric model of guided waves,[29] we can express this with the following equations:

$$\Delta t_{max} = \frac{L}{c\sqrt{(1 - \mathrm{NA}^2)}}(n_2 + n_1) \tag{9}$$

$$\Delta t_{min} = \frac{L}{c}(n_2 + n_1) \tag{10}$$

where Δt_{min} = 60.9 ns and Δt_{max} = 66.4 ns, which is in agreement with the measured time. Choosing a time window of 10 ns by division allows a characterization of the fiber fluorescence. In practice, photobiochemical signals take place in a narrow time window close to the exit fluorescence. With a time window (1 ns by division), the noise is reduced to the fluorescence generated at the end of fiber in contact with the measured media. This fluorescence at 415-nm emission wavelength kept the same decay time with the use of different media (even in air). By time-resolved fluorescence, the single-fiber configuration can be used to optimize the FOCS, especially if detectability is the main goal. In order to measure 5-HT, a major difference of the extrinsic FOCS with respect to the voltammetric and dialysis methods is the reliance upon the different types of interactions between the tissue and apparatus. Voltammetric interactions between electrons and 5-hydroxyindole compounds either in tissue or in a bath of an electrode[30] involve the surface of an electrode. For dialysis methods, interactions between 5-HT of an extracellular liquid and dialysat are through a membrane and are also limited to the surface. For the extrinsic FOCS used *in vivo*, the nature of the interactions between endogenous 5-HT (intracellular and extracellular compartments) and light remains to be determined.

Processing of the Signal. Figure 6 exhibits the integrated intensity of 5-HT and 5-HIAA emission fluorescences collected in the same time window vs. concentration of each compound. The difference of emission fluorescence measured through our FOCS appears between these two compounds. For the same signal (integrated intensity), the concentration of 5-HT is around twenty times more than that of 5-HIAA. With 415 nm as the emission wavelength, and a bandwidth of 4 nm, 5 μM for 5-HT and 100 μM for 5-HIAA are the concentration limits determined with the use of the integrated fluorescence signal. It is well known that the normal baselines of extracellular endogenous 5-HT and 5-HIAA in the brain are in the range of 1 nM to 100 nM and 100 nM to 5 μM, respectively.[31] At the present stage of development of our system, the sensitivity level is not yet adequate for *in vivo* brain measurements of endogenous 5-HT. Further improvements by typically two orders of magnitude are therefore needed.

The simplest way to overcome this difficulty would be to adopt a double-fiber configuration (as already studied in other groups at longer wavelength[7]). Indeed, the major difficulties arising from the parasitic signal generated at the fiber tips and from the fluorescence generated along the fiber by the UV excitation beam (see Fig. 5) would be solved. Nevertheless, we believe that large improvements are possible with the use of the single-fiber configuration, which remains a more satisfactory geometry for future *in vivo* applications (i.e., in terms of probe size and reliability). The first improvement may actually come from the fiber itself, which may imply even the use of specially developed ones. If we look first at the transmission itself, it will remain in the best case limited by the Rayleigh scattering. Quartz et Silice gives an experimental attenuation coefficient (α) at 350 and 300 nm equal to 120 and 250 dB/Km, respectively. By interpolation we take an attenuation coefficient of 160 dB/Km at 337 nm. The Rayleigh diffusion is expressed by: $T = 0.8\lambda^{-4}$ with T in dB/Km and λ in μm. The theoretical attenuation is therefore equal to 62 dB/Km at 337 nm. For six meters of PCS 1000, the formula $\frac{I(x)}{I_0} = 10^{-\alpha x/10}$ gives an experimental transmission of 80% and a theoretical transmission of 92% at 337 nm (I_0 is the initial flux of photon, $I(x)$ is the transmitted flux of photon

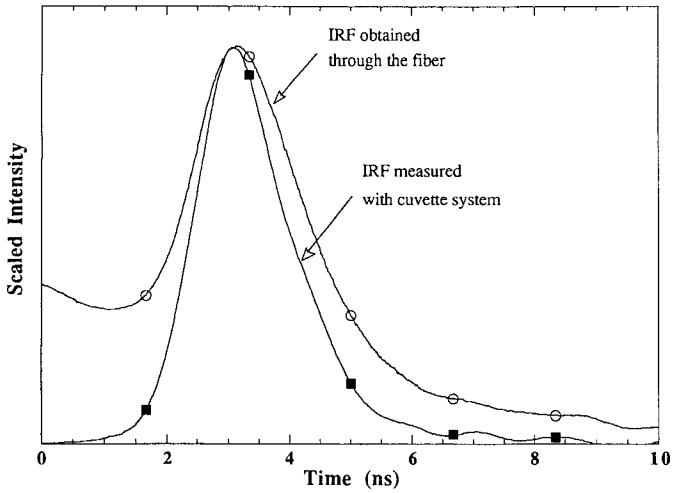

FIG. 7. Instrument response functions (IRF) at a wavelength of 337 nm.

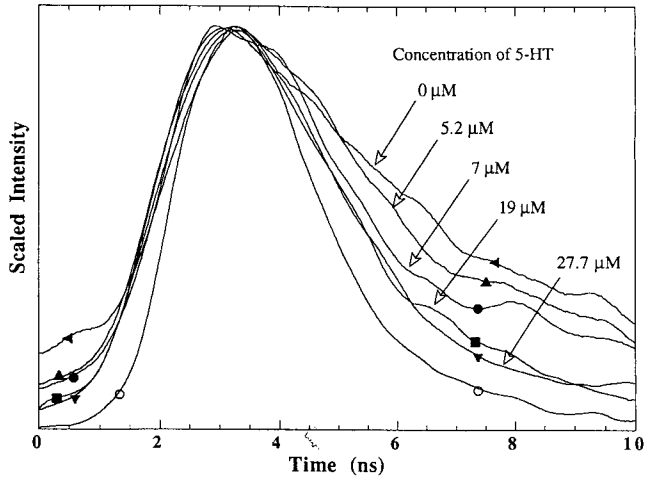

FIG. 8. Scaled fluorescence responses of 5-HT in the Merck buffer at pH 7. The curve with the white symbol is obtained with 5-HT in a cuvette at 430 nm. Other pulses come from fluorescence of 5-HT at 415 nm collected with the single-fiber configuration.

through x Km of optical fiber). Therefore, transmission fiber improvement does not appear critical, but it would lead in principle to a fiber fluorescence reduction. In fact one of the main improvements would consist in using a fiber having a much more reduced cladding fluorescence. A factor of more than one order of magnitude seems attainable.

Preliminary tests of other fused-silica fibers with high transmission properties in the UV, with low-fluorescence fused-silica cladding, are now in progress. In particular it seems that looking at fibers having a numerical aperture of 0.2 greatly widens the choice. Such a choice is not well suited to an optimal injection. Actually the nitrogen laser beam quality is rather poor and the large divergence (>10 mrad) is not adapted to a "silent" injection. This observation has been checked with the use of a much better collimated beam (YAG + harmonics divergence < 1 mrad), which nevertheless is not adapted from the point of view of time resolution. In addition it has been pointed out that the 337-nm nitrogen laser wavelength is not optimal and that a 325-nm excitation wavelength must increase the signal-to-noise ratio by a combining a high-quality tunable subnanosecond UV laser beam with high-quality fibers would be sufficient to reach an *in vivo* capability of the system. Further improvements towards short-wavelength pulsed laser diodes could be an interesting alternative in the near future.

Time-resolved fluorescence methods allow, in principle, a more refined signal analysis than integrated intensity. Temporal data lead to another parameter: fluorescence lifetime. In practice, the fluorescence response is temporally shifted as compared to the IRF, essentially because of the temporal chromatic shift. This factor forces us to move fluorescence responses forward in order to start with an identical time origin. The IRF was taken at 337 nm by measuring backscattered light. This was done by tuning the monochromator at 337 nm. No particles were added to increase scattering. Complications appear when measuring the IRF by reflection of the laser light at the fiber tip (i.e., band broadening, as reported in Fig. 7). The IRF therefore cannot be registered systematically before and after each measurement. To extract the lifetime from our signal, we used an IRF registered with the cuvette system, which does not suffer from the above-mentioned drawback. This approach may decrease the accuracy of lifetime results because we did not take into account possible slight time variations of the electronics. If accurate lifetime must be measured with our system, the method of internal calibration with the use of reference lifetimes of POPOP (p-bis[2-(5-phenyloxazolyl)] benzene) or PPO (2,5-diphenyloxazole) could be applied.[32]

Emission fluorescence pulses collected with a single fiber are presented in Fig. 8. We have scaled some fluorescence pulses in order to show temporal difference from noise (corresponding to the signal registered for buffer alone) to the fluorescence signal with various 5-HT concentrations. With 415 nm as the emission wavelength and 4 nm as the bandwidth, experimental lifetimes for 5-HT (27.7 μM) and 5-HIAA (200 μM) are 2 ns and 3 ns, respectively. These apparent lifetimes are therefore longer than those measured in the cuvette. Our principal aim when using optical fibers is not to measure with accuracy the lifetime fluorescence of 5-HT but, rather, to extract from the signal an evaluation of the lifetime range, in addition to its integration, giving qualitative information. This method is expected to be an efficient tool for *in vivo* signal identification.

The *in vivo* application has been initiated. Fluorescence (excitation wavelength: 337 nm; emission wavelengths: 390 to 530 nm) in the cortex and in deep tissue of unanesthetized rats has been actually observed. Chemical dependence of such an *in vivo* signal is now under determination. The results will be published elsewhere.[33] Our technique seems to be powerful and promising for developing a FOCS adapted to perform biochemical analysis in the brain.

CONCLUSIONS

The static fluorescence emission spectra at different excitation wavelengths, the analysis of the lifetimes, and the fractional weighting factors vs. excitation wavelengths for the use of a flashlamp TCSPC system estab-

lish the existence of two emitting states for 5-HT; the first emits at around 390 nm with a lifetime near 1 ns, and the other (well-known) emits at 340 nm with a lifetime of 2.7 ns.

With our time-resolved laser fluorometer, we show the feasibility of a FOCS for 5-HT determination. The specificity of the measurement is based on three parameters: the excitation wavelengths, the emission wavelengths, and the range of fluorescence lifetime. No signal has been observed for indole compounds such as tryptamine. 5-HT and 5-HIAA give a fluorescence signal with the same spectral properties, but their fluorescence lifetimes are different. In addition, the 390-nm fluorescence of 5-HT is twenty times more intense than that of 5-HIAA, which could permit measurements of 5-HT in the presence of 5-HIAA with a ratio of up to one thousand. With only the integrated fluorescence intensity, the detection limit of 5-HT of our FOCS is in the range of 5 μM. Noise limits our detectability and depends mainly on technical choices such as the excitation wavelength and the single-fiber configuration. Moreover, the optical fiber model choice appears to be critical, and therefore improvements may be expected. Normal baselines of extracellular endogenous 5-HT and 5-HIAA in the brain are known to be in the range of 1 nM to 100 nM and 100 nM to 5 μM, respectively. Further improvements to our system are necessary in order to increase the signal-to-noise ratio by one hundred times. The main drawback of our choices for the determination of 5-HT is the low value of the molar extinction of 5-hydroxyindole compounds at the nitrogen laser excitation wavelength used. Another subnanosecond source emitting near 320 nm would allow a better detection limit.

In addition to the characterization of two emission states of 5-HT (excitation and emission wavelengths and lifetimes), this paper demonstrates the capability of our method as an extrinsic FOCS for the *in vitro* determination of 5-HT within less than thirty seconds. We describe our investigation to solve the specific problems occurring by the use of a single-fiber configuration at an excitation wavelength in the near-UV range. In practice, the benefit of using a time-resolved fluorescence method to develop a FOCS is clearly demonstrated.

ACKNOWLEDGMENTS

The authors wish to thank Professor J. C. Talbot for his interest in this work and for making the flashlamp fluorometer available. This work was partly supported by DRET (Contract 87-215). Registry numbers: 5-HT, 153-98-0; 5-HIAA, 54-16-0; Tryptamine, 343-94-2.

1. M. Sallanon, M. Denoyer, and M. Jouvet, in *Etats de Veille et de Sommeil,* P. Meyer, J. L. Elghozi, and A. Q. Salva, Eds. (Masson, Paris, 1989), pp. 36–47.
2. J. L. Ponchon, R. Cespuglio, F. Gonon, M. Jouvet, and J. F. Pujol, Anal. Chem. **51,** 1483 (1979).
3. T. Sharp, T. Zetterström, L. Christmanson, and U. Ungerstedt, Neurosci. Lett. **72,** 320 (1986).
4. P. Kalen, E. Strecker, E. Rosengren, and A. Björklund, J. Neurochem. **5,** 1422 (1988).
5. R. Cespuglio, N. Sarda, A. Gharib, H. Faradji, and N. Chastrette, Exp. Brain Res. **64,** 589 (1986).
6. *Neuropharmacology of Serotonin,* A. R. Green, Ed. (Oxford University Press, Oxford, 1985), pp. 218 and 414.
7. J. Louch and J. D. Ingle, Anal. Chem. **60,** 2537 (1988).
8. *Application of Time-resolved Optical Spectroscopy,* V. Brüchner and K. H. Feller, Eds. (Elsevier, Amsterdam, 1990), Chaps. 3–5.
9. G. M. Hieftje and G. R. Haugen, Anal. Chim. Acta **123,** 255 (1981).
10. F. V. Bright and K. S. Litwiler, Anal. Chem. **61,** 1510 (1989).
11. T. Matsui, K. Suzuki, M. Sakagami, and T. Kitamori, Appl. Spectrosc. **45,** 32 (1991).
12. Y. Kawabata, T. Imasaka, and N. Ishibashi, Anal. Chim. Acta **173,** 367 (1985).
13. M. K. Carroll, F. V. Bright, and G. M. Hieftje, Anal. Chem. **61,** 1768 (1989).
14. M. E. Lippish, J. Pusterhofer, M. J. P. Leiner, and O. S. Wolfbeis, Anal. Chim. Acta **205,** 1 (1988).
15. D. J. Desilets, J. T. Coburn, D. A. Lantrip, P. T. Kissinger, and F. E. Lytle, Anal. Chem. **58,** 1123 (1986).
16. S. A. Nowak, F. Basile, J. T. Kivi, and F. E. Lytle, Appl. Spectrosc. **45,** 1026 (1991).
17. N. Glasser, "Transitions Radiatives et Non Radiatives dans l'Indole et ses Dérivés," Thesis, University Louis Pasteur, Strasbourg, France (1979), pp. 15–17.
18. J. R. Platt, J. Chem. Phys. **17,** 484 (1949).
19. S. Udenfriend, D. F. Bogdanski, and H. Weissbach, Science **122,** 32 (1955).
20. S. Udenfriend, D. F. Bogdanski, and H. Weissbach, Science **122,** 972 (1955).
21. R. F. Chen, Proc. Nat. Acad. Sci. USA **60,** 598 (1968).
22. G. H. Vickers, R. M. Miller, and G. M. Hieftje, Anal. Chim. Acta **192,** 145 (1987).
23. D. V. O'Connor and D. Phillips, *Time-correlated Single Photon Counting* (Academic Press, London, 1984), p. 172.
24. A. Grinvald and I. Z. Steinberg, Anal. Biochem. **59,** 583 (1974).
25. L. P. Hart and M. Daniels, Appl. Spectrosc. **46,** 191 (1992).
26. M. K. Carrol and G. M. Hieftje, Appl. Spectrosc. **45,** 1053 (1991).
27. E. R. Carraway, J. N. Demas, and B. A. Degraff, Anal. Chem. **63,** 332 (1991).
28. R. F. Chen, G. G. Vurek, and N. Alexander, Science **156,** 949 (1967).
29. A. W. Snyder and J. D. Love, *Optical Waveguide Theory* (Chapman and Hall, London, 1983), p. 32.
30. R. Cespuglio, H. Faradji, Z. Hahn, and M. Jouvet, in *Measurement of Neurotransmitter Release In Vivo,* C. A. Marsden, Ed. (John Wiley and Sons, Chichester, 1984), pp. 173–191.
31. N. T. Maidment, C. Routledge, K. F. Martin, M. Brazell, and C. A. Marsden, in *Monitoring Neurotransmitter Release during Behavior,* M. F. Joseph and M. Fillenz, Eds. (Ellis Harwood Health Sciences Series, Chichester, 1986), pp. 73–93.
32. F. Castelli, Rev. Sci. Instrum. **56,** 538 (1985).
33. S. Mottin, C. Tran-Minh, P. Laporte, R. Cespuglio, and M. Jouvet, paper delivered at the 14th International Conference IEEE Engineering in Medicine and Biology Society, Lyon, France (1992), pp. 235–238.